Laser-ablation ICP-MS analysis of silicate and sulfide melt inclusions in an andesitic complex II

Evidence for magma mixing and magma chamber evolution

Originally published in:
Contributions to Mineralogy and Petrology 147(4), https://doi.org/10.1007/s00410-004-0563-5

Contrib Mineral Petrol (2004) 147: 397–412
DOI 10.1007/s00410-004-0563-5

ORIGINAL PAPER

Werner E. Halter · Christoph A. Heinrich
Thomas Pettke

Laser-ablation ICP-MS analysis of silicate and sulfide melt inclusions in an andesitic complex II: evidence for magma mixing and magma chamber evolution

Received: 17 December 2002 / Accepted: 16 January 2004 / Published online: 6 April 2004

Abstract Laser-ablation microanalysis of a large suite of silicate and sulfide melt inclusions from the deeply eroded, Cu-Au-mineralizing Farallón Negro Volcanic Complex (NW Argentina) shows that most phenocrysts in a given rock sample were not formed in equilibrium with each other. Phenocrysts in the andesitic volcano were brought together in dominantly andesitic—dacitic extrusive and intrusive rocks by intense magma mixing. This hybridization process is not apparent from macroscopic mingling textures, but is clearly recorded by systematically contrasting melt inclusions in different minerals from a given sample. Amphibole (and rare pyroxene) phenocrysts consistently contain inclusions of a mafic melt from which they crystallized before and during magma mixing. Most plagioclase and quartz phenocrysts contain melt inclusions of more felsic composition than the host rock. The endmember components of this mixing process are a rhyodacite magma with a likely crustal component, and a very mafic mantle-derived magma similar in composition to lamprophyre dykes emplaced early in the evolution of the complex. The resulting magmas are dominantly andesitic, in sharp contrast to the prominently bimodal distribution of mafic and felsic melts recorded by the inclusions. These results severely limit the use of mineral assemblages to derive information on the conditions of magma formation. Observed mineral associations are primarily the result of the mixing of partially crystallized magmas. The most mafic melt is trapped only in amphibole, suggesting pressures exceeding 350 MPa, temperatures of around 1,000 °C and water contents in excess on 6 wt%. Upon mixing, amphibole crystallized with plagioclase from andesitic magma in the source region of porphyry intrusions at 250 MPa, 950 °C and water contents of 5.5 wt%. During ascent of the extrusive magmas, pyroxene and plagioclase crystallized together, as a result of magma degassing at low pressures (150 MPa). Protracted extrusive activity built a large stratovolcano over the total lifetime of the magmatic complex (> 3 m.y.). The mixing process probably triggered eruptions as a result of volatile exsolution.

Editorial responsibility: T.L. Grove

Electronic Supplementary Material Supplementary material (eTable 1and eFigure 1) is available for this article if you access the article at http://dx.doi.org/10.1007/s00410-004-0563-5. A link in the frame on the left on that page takes you directly to the supplementary material.

W. E. Halter (✉) · C. A. Heinrich · T. Pettke
Department of Earth Sciences, Isotope Geochemistry and Mineral Resources, ETH Zurich,
8092 Zurich, Switzerland
E-mail: halter@erdw.ethz.ch
Tel.: +41-1-6326802
Fax: +41-1-6321827

Introduction

Mafic enclaves in felsic rocks and other petrographic and petrologic evidence (e.g. Mandeville et al. 1996; Wolf and Eichelberger 1997; Coombs et al. 2000; Cole et al. 2001) suggest that andesitic magmas commonly involve mixing of acid and mafic melts. This mixing can lead to magmatic volatile saturation, which can potentially trigger volcanic eruptions (Hattori 1993) and may play a decisive role in the formation of magmatic-hydrothermal ore deposits (Dietrich et al. 1999). Complete mixing or "hybridization" (Sparks and Marshall 1986) is much less apparent and might often escape recognition in geological and geochemical studies. The mixing process may occur by injection of basic melt into an evolved magma reservoir where the distinct melts mix prior to eruption (Wolf and Eichelberger 1997; Venezky and Rutherford 1997). It may also occur during eruption of a structured magma chamber containing compositionally distinct regions (Sigurdsson and Sparks 1981; Druitt and Bacon 1989; Jaupart and Tait 1990; Mandeville et al. 1996; Cole et al. 2001), or by continued supply of distinct magmas without formation of a major

magma chamber (Dungan et al. 2001). Distinguishing these processes is essential for a better understanding of the genesis of andesitic rocks in general, for predicting the causes and mechanisms of eruption and emplacement of subvolcanic stocks (Tait et al. 1989; Kress 1997; Matthews et al. 1997; Stix et al. 1997; Murphy et al. 2000), and for identifying the specific conditions required for the formation of magmatic-hydrothermal ore deposits (Dilles 1987; Cline and Bodnar 1991).

With this motivation, we have studied the geology, geochronology, element and radiogenic isotope geochemistry of the Farallón Negro Volcanic Complex, a large Miocene calcalkaline volcano in the Andes of NW Argentina (Llambias 1970; Sasso 1997; Halter et al. 2004a). This complex is composed of a large stratovolcano, eroded to its base and exposing numerous subvolcanic intrusions. One of these stocks hosts the world-class Bajo de la Alumbrera porphyry-Cu-Au deposit (Proffett 1995; Ulrich and Heinrich 2002). Our integrated project aims at reconstructing the magma evolution of the entire long-lived andesitic complex. Of particular interest are the genetic relations between extrusive rocks and co-magmatic intrusions. In previous studies we have established the chemical evolution and isotope geochemistry of the complex (Halter et al. 2004a), and we have established and tested laser-ablation inductively-coupled-plasma mass-spectrometry (LA-ICPMS) for the quantitative analysis of melt inclusions (Halter et al. 2002b; Halter et al. 2004b). A key advantage of this technique is the possibility to efficiently analyze entire crystallized silicate and sulfide melt inclusions without prior thermal re-homogenization. In this paper, we integrate the earlier results with a large dataset of microanalyses of melt inclusions, spanning all extrusive and intrusive stages in the evolution of the Farallón Negro Volcanic Complex. The new results are considered equally significant for hydrothermal ore formation as for the origin of andesites and the evolution of calcalkaline magma chambers in general.

Geological setting

The Farallón Negro Volcanic Complex (FNVC) is located in the Hualfin District of the Catamarca Province in northwestern Argentina. It is the easternmost manifestation of Late Tertiary volcanic activity in the area (~200 km east of the present volcanic arc) and lies in the Sierras Pampeanas province, close to the southwestern margin of the Puna physiographic and tectonic province (Fig. 1). The contact between these two provinces is marked by the NE–SW-striking crustal-scale Tucuman Transfer Zone (Urreiztieta et al. 1993), which probably controlled magma ascent along local dilatancies (Sasso 1997). The Sierras Pampeanas are dominated by broad regions of basement uplift forming kilometer-scale blocks (Jordan and Allmendinger 1986; Allmendinger 1986). Uplift occurred as a result of westward migrating deformation since the late Miocene (Coughlin et al. 1998). Associated reverse faults subdivided the FNVC into several zones separated by basement rocks, exposing volcanic and subvolcanic intrusive rocks at variable levels.

Previous mapping and analysis of this system (Llambias 1970; Sasso 1997; Halter et al. 2004a) shows that the complex consists of the remnants of a 20-km-wide stratocone, intruded by numerous subvolcanic stocks (Fig. 2). Volcanic units dip away from a large central stock (Alto de la Blenda) such that the present erosion level allows continuous sampling of the entire volcanic pile (Halter et al. 2004a). The present study focuses on the northwestern sector of the complex, which records most of the intrusive and hydrothermal events, including the formation of the large Bajo de la Alumbrera porphyry Cu-Au deposit.

Evolution of the magmatic complex

Based on extensive field observations (including several mapped transects), whole rock geochemistry, isotopic and geochronologic data, we have reconstructed the evolution of the FNVC (Fig. 3) from the beginning of volcanism at 9.7 Ma to the last subvolcanic intrusion emplaced at 6.1 Ma (Halter et al. 2004a).

The oldest volcanic rocks are high potassium calcalkaline basalts, basaltic andesites and andesites, with SiO_2contents between 45 and 66 wt% and phenocryst assemblages of amphibole + plagioclase + magnetite ± pyroxene (10–15, 20–30, 5–7 and 10–20 vol%, respectively, in the most mafic magmas). The matrices are fine grained and consist mainly of plagioclase microlites. Variations in the chemical and mineralogical compositions of magma is observed from flow to flow, but no long-term evolution is apparent in the volcanic stratigraphy. The central Alto de la Blenda stock is considered as the principal conduit for the volcanic rocks, and its crystallization ended the main extrusive activity at 7.5 Ma. The youngest volcanic rocks are present in the northwestern part of the system, where biotite and quartz-phyric dacitic breccias erupted at 7.35 Ma. Coeval dacitic intrusions, emplaced at Agua Tapada, are considered as feeders in a flank eruption. This event is associated with a partial collapse of a caldera in the northwestern part of the complex (Halter et al. 2004a).

Subvolcanic stocks first emplaced at 9.0 Ma become abundant only after 8.5 Ma. Individual stocks are formed of one to nine intrusions, emplaced within a restricted time frame, but comprising a wide range in compositions. Stocks contain amphibole + plagioclase + magnetite ± pyroxene or plagioclase + magnetite ± amphibole ± biotite as the main phenocryst assemblages. Pyroxene is restricted to early intrusions and represents at most 10 vol% of phenocrysts. Biotite appears as a major phenocryst phase in intrusions after 7.5 Ma. Amphibole is an abundant phenocryst in most intrusive stocks, except in the latest and most silica-rich intrusions, in which biotite is the dominant mafic phase. Most

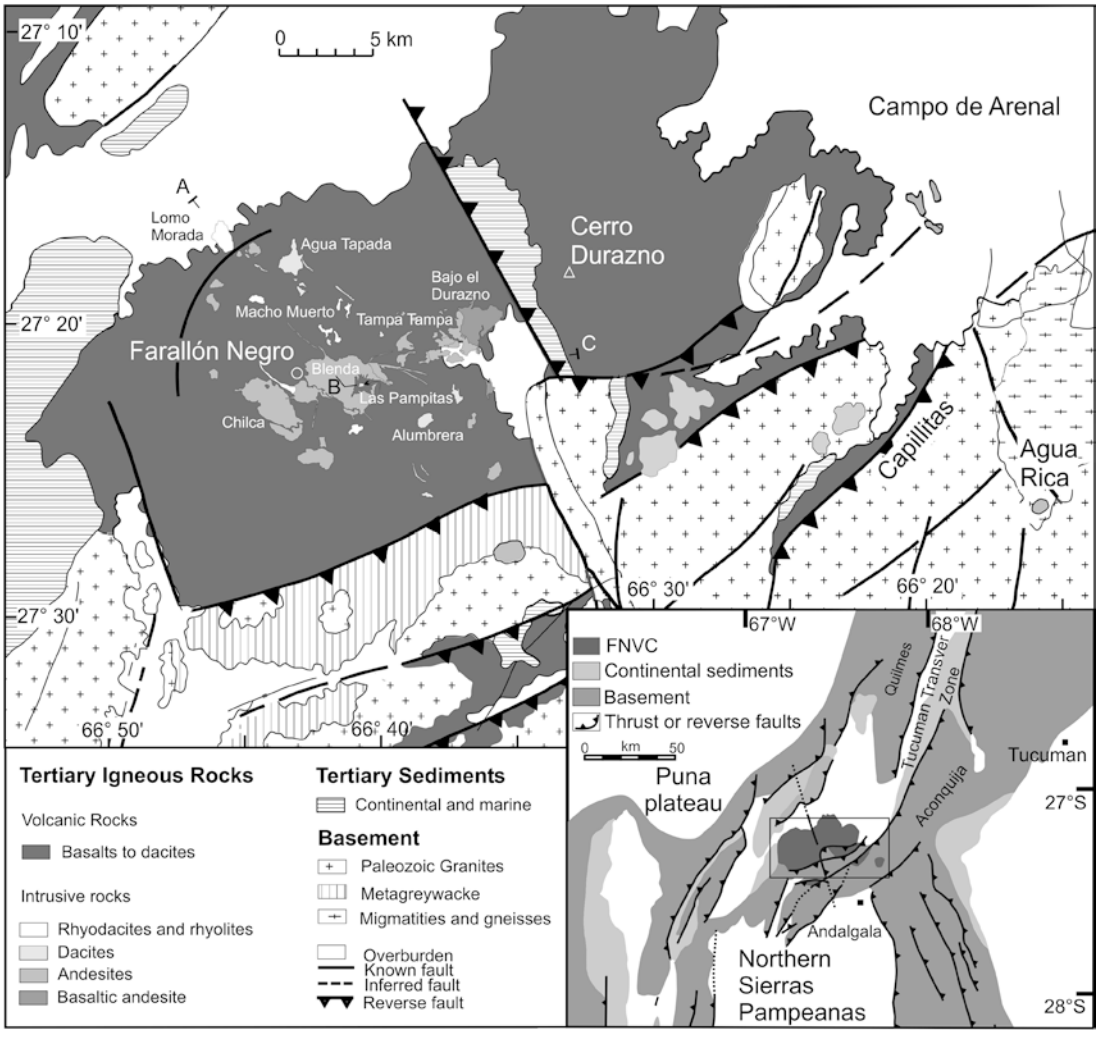

Fig. 1 Simplified geological map of the Farallón Negro Volcanic Complex in northwestern Argentina (Llambias 1970, 1972; Martinez et al. 1995). The *inset* shows the location of the complex on the Tucuman transfer zone, between the Puna plateau and the Sierras Pampeanas. The andesitic stratocone is eroded to a plane section, some 5,000 m below the original summit. Numerous subvolcanic intrusions crop out at this erosion level. *A*, *B*, *C* represent the approximate trace of the schematic cross section of Fig. 3

mafic rocks contain only little plagioclase phenocrysts, which is the dominant phenocryst in dacites and rhyodacites.

Shortly after the cessation of the volcanic activity a dacitic intrusion was emplaced at Las Pampitas (7.2 Ma). Emplacement of the Bajo de la Alumbrera stock started about 0.4 Ma after the main volcanic activity had ceased. It formed between 7.1 and 6.7 Ma as a series of nine mappable intrusions showing a continuous evolution from early silica-rich dacites to late intermediate andesites (Proffett 1995; Ulrich and Heinrich 2002). Deep drill cores show textural evidence for mingling between dacitic and andesitic magmas (phenocrysts growing across the interface; Halter et al. 2004a). Pervasive alteration affects all early intrusions at Alumbrera, and intense veining, potassic alteration and Cu-Au mineralization is associated with the 2nd to 4th intrusive events. Late andesitic intrusions in this stock are unaltered and barren. Small rhyodacite and rhyolite stocks, emplaced after the Alumbrera stock, are the last recorded signs of magmatic activity in the Farallón Negro district. In contrast to all the previous stocks, these rocks are essentially unaltered.

Although compositional evolution is towards more mafic compositions in individual stocks, the most silica-rich intrusions of each stock define a continuous trend of increasing SiO_2content between 8.5 and 6.1 Ma (Fig. 3). This systematic evolution was not related to any spatial distribution, as intrusions were emplaced randomly around the central Alto de la Blenda stock but rather suggests that intrusions were derived from a subvolcanic magma chamber, which evolved between 8.5 and 6.1 Ma. This reservoir could only remain molten by a sustained heat input by fresh magma (Halter et al. 2004a).

Mineralogical, isotopic and major to trace element compositions of intrusive and extrusive rocks overlap across a wide range of compositions. The only apparent difference is that intrusive rocks evolve to higher silica contents after the volcanic activity had ceased. The

Fig. 2 Overview of part of the Farallón Negro Volcanic Complex, looking ESE from the Agua Tapada area. Apparent are the volcanic rocks and the strongly sericitized Agua Tapada intrusion in the front. Sediments at the base of the Cerro Durazno volcanics (the prominent escarpment in the background) are exposed as a result of uplift along a reverse NNW–SSE-trending fault (see Fig. 1)

chemical and isotopic similarity and the spatial and temporal overlap suggest that intrusive and extrusive rocks are co-magmatic. Concentrations of all major and most trace elements lie on the same linear trends when plotted against SiO_2 (Halter et al. 2004a). Such linear trends and linear correlations between element enriched in felsic melts (e.g., Na) and elements enriched in mafic melts (e.g. Ti) are consistent with a dominantly binary mixing between a silica-rich and a silica-poor magma, rather than fractional crystallization (Halter et al. 2004a).

LA-ICPMS analyses of minerals and melt inclusions

Silicate melt inclusions are trapped in amphibole, pyroxene, plagioclase and quartz in intrusive and extrusive rocks. These inclusions are generally crystallized or contain daughter phases in glassy matrices. Gas bubbles constituting 10 to 30% of the total volume can be recognized in the least crystallized inclusions. Descriptions of melt inclusion textures are given in the companion paper by Halter et al. (2004b), along with all analytical aspects of their investigation. Melt inclusions in mafic phases and quartz were mainly trapped during continuous growth of the crystals. Inclusions in plagioclase were generally trapped along growth zones, possibly following events of partial resorption of the phenocrysts. In late intrusions, such melt inclusions can be very large, and many of them were trapped at the same time as numerous inclusions of biotite and magnetite occurring in the same growth zone (e.g., sample NB9–9, Fig. 4A). Inclusions in plagioclase, itself hosted by an amphibole have rarely been encountered but analyzed where possible (Fig. 4B). Inclusions were analyzed in selected samples throughout the volcanic pile and in all the intrusions named in

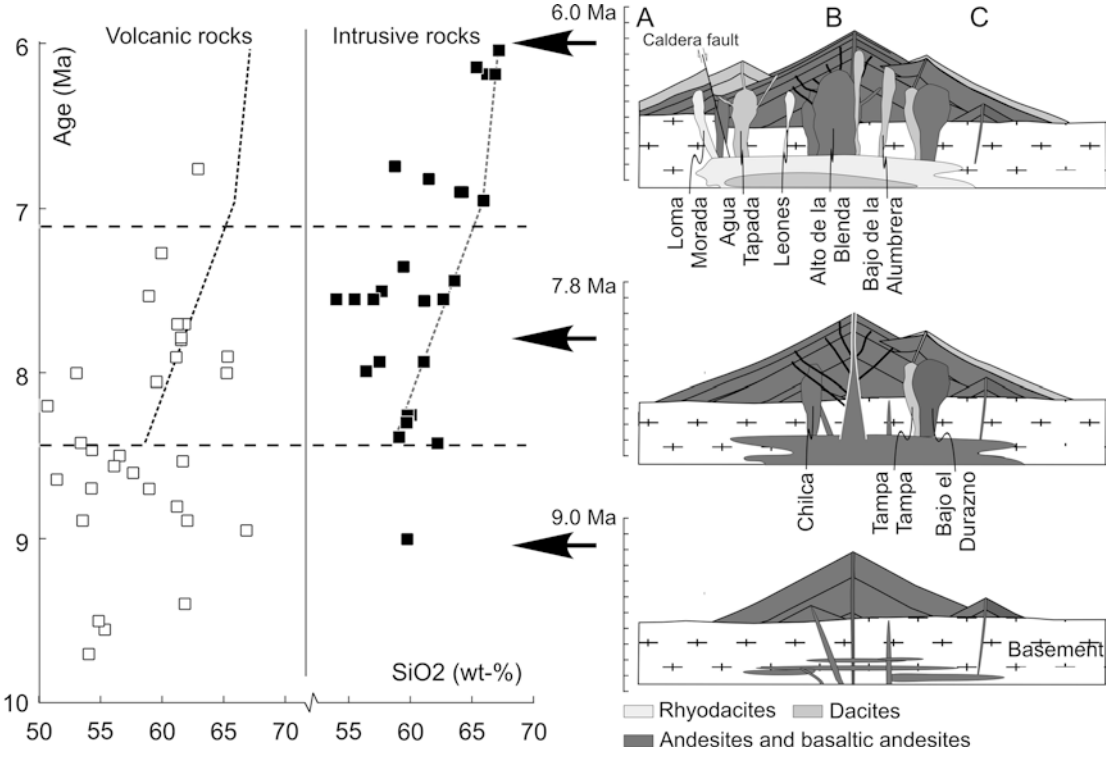

Fig. 3 The sequence of events in the FNVC is based on detailed mapping, age dating and analytical data (Halter et al. 2004a and references therein). See text for details on the evolution of the magmatic systems. The *dashed line* connects the most silica-rich intrusions and suggests a continuous evolution of the system, possibly in a long-lasting magma chamber. The approximate location of the cross section *A*, *B* , *C* is shown in Fig. 1

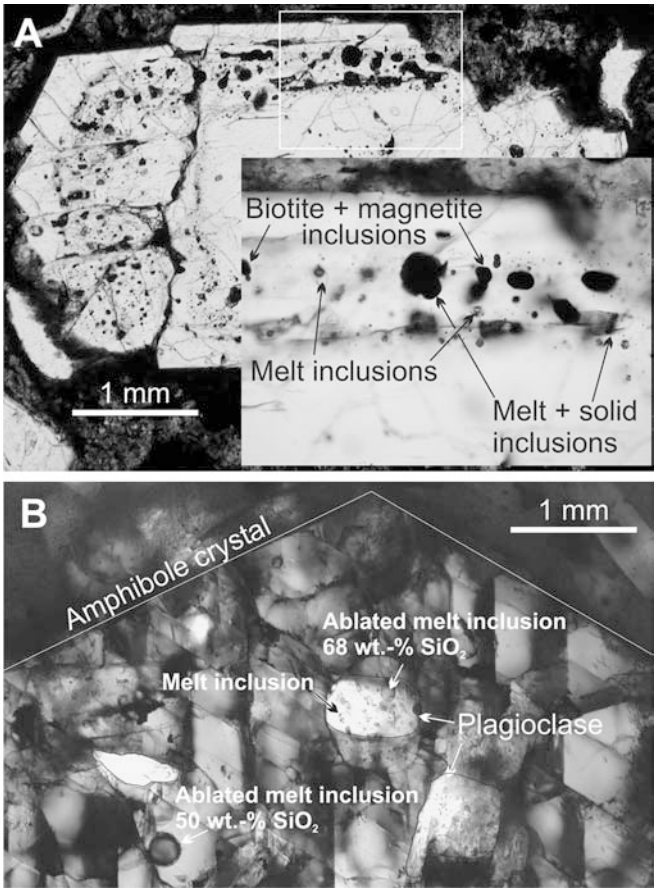

Fig. 4 **A**Microphotograph of a plagioclase crystal in the late Loma Morada intrusion. Growth zones with highly irregularly shaped melt inclusions, trapped concurrently with numerous solid phases suggest rapid growth, possibly through volatile loss. **B** Plagioclase inclusions in amphibole, each hosting silicate melt inclusions

Fig. 1. A brief description of each sample is given in Table 1.

Analyses were conducted using laser-ablation inductively-coupled-plasma mass-spectrometry (LA-ICPMS) of entire glassy and crystallized inclusions without prior homogenization or exposure to the sample surface, using the signal de-convolution and quantification procedure of Halter et al. (2002b) and Heinrich et al. (2003). The average water content of silicate melt inclusions was assumed to be 4 wt %; a variation of ± 2 wt % of this water content would affect the results by the same percentage, which is well below the uncertainty of the calculated element concentrations. Tests of the accuracy of this analytical approach with regard to this study are discussed in Halter et al. (2004b) and Pettke et al. (2002), showing that melt inclusions are accurately quantified and representative of the bulk melt compositions from which the phenocrysts grew. In particular, we tested that correct results are obtained for compositionally identical inclusions in different, but petrographically co-existing host phases (Halter et al. 2004b). Only the Fe and Mg underwent some post-entrapment re-equilibration in inclusions trapped in mafic minerals, and these elements are not further used in the interpretation. All analyses of inclusions and their hosts are provided in eTable 1 as a data repository.

Mineral compositions

Representative compositions of the main host phenocryst phases for melt inclusions are shown in Table 2, and the range of element concentrations in these minerals are contoured in Fig. 5. Pyroxene is mostly

Table 1 Samples used for melt inclusion analysis

Sample	Location	Rock	Main phenocrysts	Melt inclusions hosts	Age (Ma)
Volcanic rocks					
NB 5A (99)	Agua Tapada	Basaltic andesite	Plagioclase, amphibole, pyroxene, spinel	Pyroxene, plagioclase	~8.0
NB 9 (99)	Agua Tapada	Andesite	Plagioclase, amphibole, pyroxene, spinel	Pyroxene, plagioclase	8.05 ± 0.37
NB 15 (99)	Agua Tapada	Andesite	Plagioclase, amphibole, spinel	Plagioclase	7.78 ± 0.28
NB 31A (99)	Agua Tapada	Basaltic andesite	Plagioclase, amphibole, pyroxene, spinel	Amphibole, pyroxene	~8.0
NB 5B (00)	Tampa Tampa	Basaltic andesite	Plagioclase, amphibole, pyroxene, spinel	Amphibole, plagioclase	~9.5
NB 6 (00)	Tampa Tampa	Andesite	Plagioclase, amphibole, pyroxene, spinel	Pyroxene, plagioclase	9.4 ± 0.3
NB 31B (00)	Tampa Tampa	Andesite	Plagioclase, amphibole, spinel	Amphibole, plagioclase	9.0 ± 0.2
NB 49 (00)	Las Pampitas	Basaltic andesite	Plagioclase, amphibole, pyroxene, spinel	Plagioclase	~9.7
22–1KL	Agua Tapada	Andesite	Plagioclase, biotite, amphibole, quartz	Plagioclase	7.37 ± 0.35
Intrusive rocks					
ML 5	Bajo el Durazno	Andesite	Plagioclase, amphibole, pyroxene, spinel	Amphibole, plagioclase	~8.2
ML 39	Las Pampitas	Dacite	Plagioclase, biotite, amphibole, quartz	Plagioclase, quartz	7.22 ± 0.28
9–9 (99)	Lomo Morado	Rhyodacite	Plagioclase, biotite, amphibole, quartz	Plagioclase	6.14 ± 0.05
ML9	Alto de la Blenda	Andesite	Plagioclase, amphibole, pyroxene, spinel	Pyroxene	7.5 ± 0.20
ML 41	Macho Muerto	Rhyodacite	Plagioclase, biotite, amphibole, quartz	Plagioclase	6.26 ± 0.15
ML44	Agua Tapada	Dacite	Plagioclase, biotite, amphibole, quartz	Plagioclase, quartz	7.39 ± 0.17
ML47	Chilca	Andesite	Plagioclase, amphibole, pyroxene, spinel	Amphibole	7.94 ± 0.11
BLA 67	Alumbrera	Andesite	Plagioclase, amphibole, spinel	Amphibole, plagioclase	6.78 ± 0.15
TU10	Alumbrera	Dacite	Plagioclase, biotite, amphibole, quartz	Quartz	6.83 ± 0.07
NB 32 (00)	Tampa Tampa	Andesite	Plagioclase, amphibole, spinel	Amphibole, plagioclase	9.0 ± 0.3

Numbers in parenthesis are the sampling years referred to in Ages are Ar-Ar ages described in Halter et al. (2004a)

Table 2 Compositon of representative melt inclusions and host minerals with one sigma uncertainties (RSD in % of the values)

Melt Inclusions								Host mineral							
	Pyroxene		Amphibole		Plagioclase		Quartz		Pyroxene		Amphibole		Plagioclase		Quartz	
SiO_2	58.95	2%	50.96	4%	70.24	2%	66.96	9%	51.32	2%	47.20	1%	60.65	1%	99.96	1%
TiO_2	0.32	5%	0.90	6%	0.18	2%	0.07	7%	0.64	2%	1.88	2%	0.0064	8%	0.011	4%
Al_2O_3	16.45	1%	16.91	3%	14.30	2%	16.51	1%	3.63	2%	9.39	1%	23.29	1%	0.023	2%
Fe_2O_3	5.91	4%	8.98	4%	0.76	2%	6.71	1%	9.61	2%	17.46	1%	0.27	2%	< 0.0024	
MnO	0.15	6%	0.14	4%	0.041	2%	0.12	1%	0.41	2%	0.28	1%	0.0063	2%	0.0001	98%
MgO	2.79	11%	5.10	4%	0.057	5%	0.40	3%	14.89	2%	10.15	1%	0.012	7%	0.0003	33%
CaO	4.04	10%	8.23	5%	3.51	3%	1.10	6%	19.14	2%	7.72	2%	9.60	1%	< 0.011	
Na_2O	3.19	1%	3.731	3%	4.71	2%	0.034	3%	0.36	2%	2.48	1%	5.64	1%	0.0012	5%
K_2O	4.20	0%	1.05	3%	2.19	1%	4.09	1%	0.0008	19%	1.44	1%	0.54	1%	< 0.0001	
Total	96.00		96.00		96.00		96.00		100.00		98.00		100.00		100.00	
Cu	67	2%	3	134%	3.2	23%	< 69		2.5	22%	< 1.8		< 0.24		< 0.777	
Zn	37	12%	112	23%	24	11%	< 236		67	5%	218	6.3%	8.5	12%	< 3.580	
Rb	129	1%	4	40%	84	2%	157	2%	< 0.05		4.3	14%	0.68	14%	< 0.050	
Sr	350	1%	797	4%	540	3%	57	3%	41	2%	164	2%	1140	1%	< 0.530	
Y	22	5%	23	15%	64	2%	16	4%	36	2%	50	4%	0.30	19%	< 0.017	
Zr	172	1%	33	18%	656	1%	65	3%	46	3%	75	5%	< 0.089		< 0.041	
Nb	16	2%	8	30%	60	2%	13	6%	0.17	32%	21	7%	< 0.052		< 0.061	
Mo	1.6	18%	< 0.67		9.2	13%	NA		0.22	71%	0.57	104%	0.092	98%	< 0.089	
Ba	464	1%	199	11%	529	2%	43	6%	0.31	45%	244	4%	211	2%	NA	
Cs	6.2	2%	< 0.16		6.4	4%	4.1	7%	< 0.02		< 0.12		< 0.036		0.025	33%
La	26	1%	8	21%	25	3%	12	4%	3.3	6%	12	7%	7.9	3%	< 0.016	
Ce	50	1%	23	13%	66	2%	23	3%	15	3%	45	4%	12	3%	0.016	35%
Nd	22	6%	19	31%	49	4%	12	10%	19	5%	42	8%	2.6	11%	< 0.215	
Yb	1.7	34%	3.9	67%	7.8	9%	NA		3.9	11%	4.1	25%	< 0.15		NA	
Ta	1.0	5%	0.7	71%	4.2	6%	NA		0.06	40%	0.40	38%	< 0.020		NA	
Pb	11.6	3%	4	55%	16	5%	37	4%	< 0.25		2.5	30%	8.8	5%	0.15	23%
Th	9.2	2%	< 0.20		64	2%	16	4%	0.06	43%	0.19	64%	< 0.0001		< 0.019	
U	2.9	3%	< 0.00		15	4%	4.6	7%	0.03	63%	< 0.12		0.021	69%	0.038	25%
MF	0.44		0.93		0.69		0.16									

Major elements are in wt%, trace elements in ppm. The water content was estimated; < 69.10 below limit of detection; *NA* not analysed; *MF* mass factor (mass of inclusion/total mass ablated); Uncertainties are one standard deviation of the analytical uncertainty

clinopyroxene; some orthopyroxene crystals were found in volcanic rocks only. Both are Fe-rich with Mg-numbers (MgO/FeO + MgO molar) between 60 and 80. Compositions of amphibole remain in the broad field of hornblende, with intermediate to Fe-rich compositions (Mg-numbers between 40 and 60 but subject to uncertainty due to partial re-equilibration) and Al_2O_3 contents between 8 and 12 wt%. Plagioclase compositions range from An_{70} in basaltic andesites to An_{25} in late rhyodacitic intrusions.

Silicate melt inclusions

Examples of typical element concentrations in melt inclusions and their 1σ analytical uncertainties in various host minerals are reported in Table 2. Results for approximately 200 individual melt inclusions in 19 samples are presented graphically for selected major and trace elements (9 elements out of 28 elements analyzed) in eFig. 1 in comparison with bulk rock compositions and plots for K, Ca, Ti and Sr is given as an example in Fig. 5. The full data set is provided in eTable 1. Melt inclusions are identified as a function of the sample and the host mineral phase in which they occur. Several inclusions per phenocryst type were analyzed in each sample and each mineral, to identify any outlie in an inclusion assemblage. Because of the large number of data and for the sake of clarity, inclusions in rocks emplaced before or after 8.5 Ma are displayed on separate diagrams.

Silicate melt inclusions have SiO_2content between 42 and 75 wt%, covering a similar compositional range as bulk rocks. Changes in the composition of melt inclusions with increasing SiO_2 content and other inter-element correlation trends follow those of bulk rocks for

►

Fig. 5 Plots of SiO_2 vs. K, Ca, Ti and Sr in individual melt inclusions (*colored symbols*), minerals (fields labeled *A*, *O*, *C* and *P* for amphibole, orthopyroxene, clinopyroxene and plagioclase, respectively), and whole rocks (*small crosses*). The data are grouped by the mode of emplacement of the host rock and in the case of K_2O for its age. Within each plot, same colors characterize inclusions from the same sample. Melt inclusion compositions generally follow the mixing trend defined by whole rocks (*thin black dashed lines*). Deviations from the mixing trend are due to crystallization of phenocrysts, without removal of solid phases. Arrow "1" represents the predicted effect of crystallization of plagioclase and pyroxene and the resorption of amphibole in a magma of intermediate composition. Arrow "2" shows the effect of plagioclase crystallization on the melt composition in a silica-rich magma. *Colored dashed lines* represent predicted effect of mixing the most mafic melt with melts in highly crystallized, silica-rich magmas

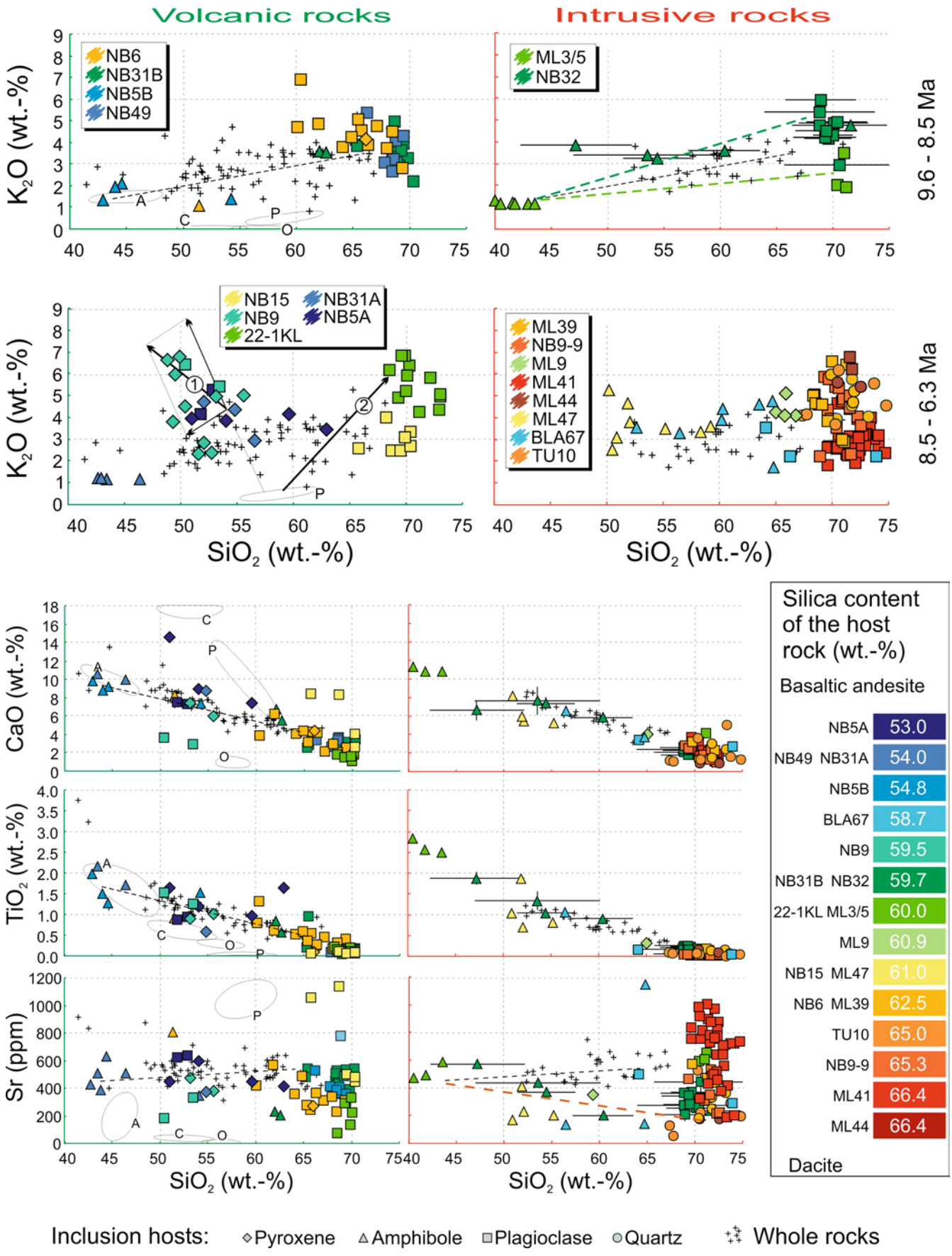
Volcanic rocks
Intrusive rocks
NB6
NB31B
NB5B
NB49
ML3/5
NB32
9.6 - 8.5 Ma
NB15
NB9
22-1KL
NB31A
NB5A
ML39
NB9-9
ML9
ML41
ML44
ML47
BLA67
TU10
8.5 - 6.3 Ma
K2O (wt.-%)
SiO2 (wt.-%)
CaO (wt.-%)
TiO2 (wt.-%)
Sr (ppm)
A
C
P
O
1
2
Silica content of the host rock (wt.-%)
Basaltic andesite
NB5A 53.0
NB49 NB31A 54.0
NB5B 54.8
BLA67 58.7
NB9 59.5
NB31B NB32 59.7
22-1KL ML3/5 60.0
ML9 60.9
NB15 ML47 61.0
NB6 ML39 62.5
TU10 65.0
NB9-9 65.3
ML41 66.4
ML44 66.4
Dacite
Inclusion hosts:
Pyroxene
Amphibole
Plagioclase
Quartz
Whole rocks

most elements (Fig. 5), except for small but diagnostic deviations observed for some elements at particular stages of the evolution (below).

The most mafic inclusions in intrusive and extrusive rocks, with SiO_2 contents between 42 and 45 wt%, occur exclusively in amphibole (samples NB5B, NB31A, ML3/5 and NB32). Figure 6 shows similar compositions of such a mafic inclusion from an intrusive rock and inclusions from extrusive rocks of various ages. This inclusion is also compared to the bulk analysis of an early lamprophyre dykes with SiO_2 contents around 42 wt% emplaced into basement rocks east of the main volcanic complex (Capillitas Valley; Fig. 1). These very low silica contents cannot be accounted for by an artifact of incorrect signal deconvolution as the amphibole has similar SiO_2 contents and addition/subtraction of an amphibole component does not change the SiO_2 content

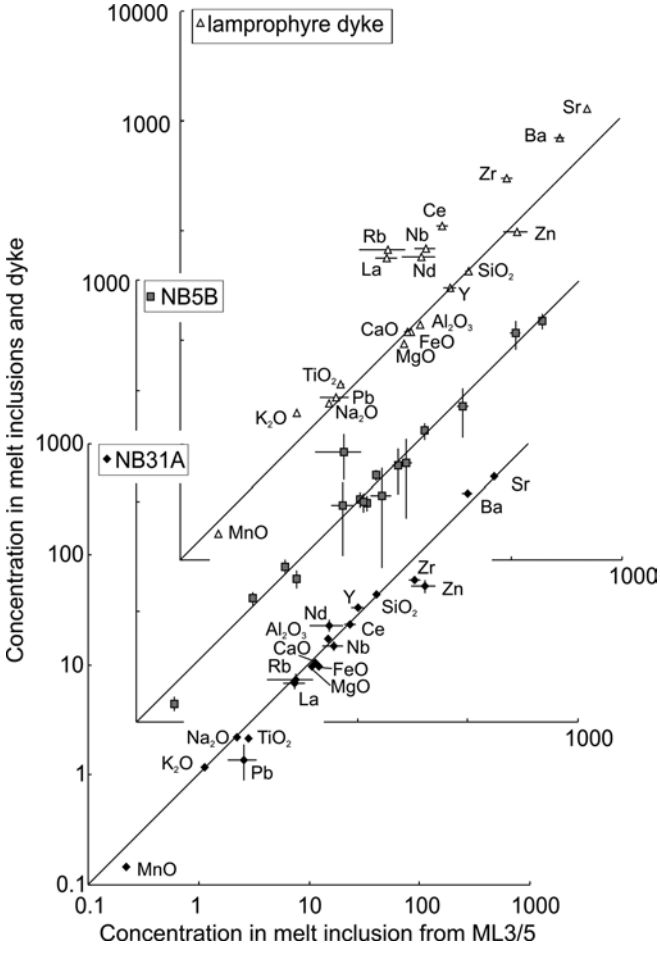

Fig. 6 Comparison between element concentrations in mafic melt inclusions trapped in amphibole from an intrusion (ML3/5) and from extrusive rocks of various ages (NB5B and NB31A). The close similarity between the compositions suggests that both rock types were generated from the same primary magma. Also shown is the comparison between the melt inclusion from sample ML3/5 and a lamprophyre dyke emplaced in the Capillitas valley (CAP 4, CAP 5; Halter et al. 2004a). This dyke has a bulk composition most similar to that of the most mafic melt inclusions and could represent the most pristine mafic magma endmember

of the calculated melt composition. Element abundances normalized to primitive mantle (Hofmann 1988) are compared in Fig. 7, showing the flattest patterns for melt inclusions and somewhat greater enrichment of the least compatible elements in lamprophyre dykes.

Inclusions with basic to intermediate SiO_2 contents between 48 and 55 wt% are found in amphibole in intrusive rocks and in amphibole, pyroxene and plagioclase in volcanic rocks. In pyroxene and plagioclase from volcanic rocks, they may depict unusual enrichments in K, Na and Rb deviating from the bulk rock trend. Pyroxene phenocrysts host melt inclusions with a restricted range in SiO_2 content between 50 and 60 wt%. These inclusions were only found in samples from volcanic rocks and in the central Alto de la Blenda stock (sample ML9). Pyroxene in other intrusive rocks is scarce and does not host any melt inclusions.

Melt inclusions with SiO_2 contents between 55 and 65 wt% are trapped in plagioclase pyroxene and amphibole in volcanic rocks, and then have similar compositions to these rocks. In contrast, inclusions of similar silica content in intrusive rocks are recorded mainly in amphiboles and show K, Rb and Y enrichments and Sr depletion relative to bulk rocks. The central Alto de la Blenda stock is the only intrusion that contains pyroxene that trapped melt inclusions with element concentrations similar to bulk rocks. Thus, they have characteristics similar to melt inclusions found in volcanic rocks.

Melts with more than 65 wt% SiO_2 are trapped almost exclusively in plagioclase and quartz. Such silica-rich inclusions are present in plagioclase from nearly all the samples, including mafic rocks emplaced very early in the evolution of the system (e.g., sample NB49 emplaced at approximately 9.5 Ma). Inclusions in plagioclase from intrusive rocks always contain more than 70 wt% SiO_2, i.e., they are richer in silica than melt inclusions in plagioclase from extrusions. The highest silica contents were measured in melt inclusions trapped by plagioclase and quartz from intrusions emplaced after 7.0 Ma. In some samples, these inclusions show enrichments in K, Na and Rb that are consistent within inclusion populations. Thus, the 7 wt% K_2O in melt inclusions from dacites truly reflects high potassium contents in some partially crystallized magmas. The most extreme compositions with the highest SiO_2 contents are found in the latest rhyodacitic intrusions.

Frequency distribution of melt inclusion and rock compositions

Although the compositional trends of bulk rocks and melt inclusions largely overlap, there is a prominent contrast in the petrographic distribution and relative frequency of melt inclusions between different rocks (Fig. 8) and between the compositions of melt inclusions in apparently coexisting phenocryst minerals in any one rock (Fig. 9).

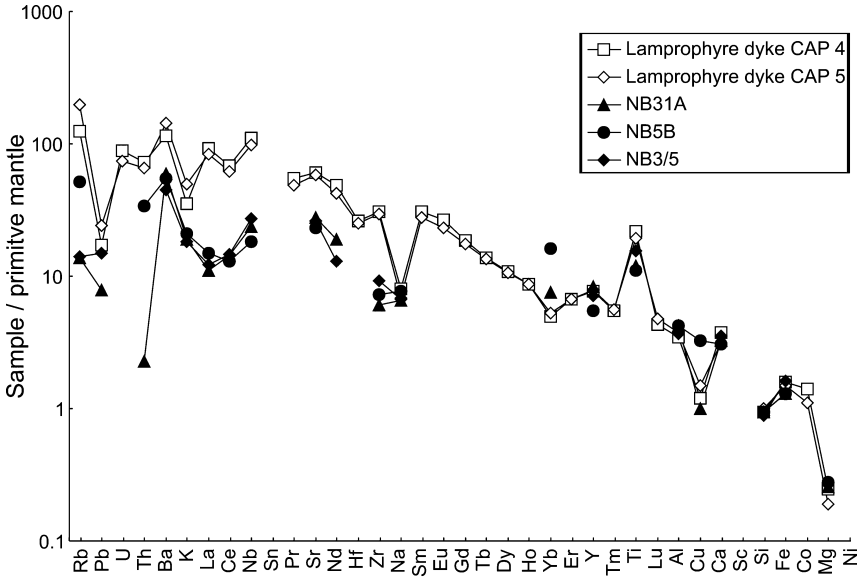

Fig. 7 Variation diagram normalized to primitive mantle (Hofmann 1988) of two lamprophyre dykes (*open symbols*; CAP 4 and CAP 5) and the most mafic melt inclusions in amphibole from intrusive and extrusive rocks (*full symbols*). Melt inclusion data suggest a more primitive pattern than that observed in lamprophyre dykes. Trace element concentrations in bulk rocks were obtained using LA-ICPMS analysis of lithium-tetraborate glass pellets

Overall, the frequency of melt inclusions with intermediate compositions (58 to 60 wt SiO_2) is low compared to the great predominance of andesitic bulk rock compositions in the Farallón Negro Volcanic Complex (Fig. 8A). The peak in intermediate bulk rock compositions is not an artifact of sampling bias; any possible bias in our field sampling would be in favor of volumetrically subordinate rocks of apparently unusual (mafic or felsic) mineralogy and bulk composition (Halter et al. 2004a).

The frequency of melt inclusions with given SiO_2 contents strongly correlates with the type of host mineral, and melt inclusions from the same sample plot in tight, yet distinct clusters. The frequency also varies somewhat with the mode of emplacement (volcanic or intrusive), but is remarkably independent of the bulk composition of the host rock. Thus, andesitic melt inclusions are completely absent from plagioclase in intrusive rocks (Fig. 8B) and rare in plagioclase from volcanic rocks (Fig. 8C). Dacitic to rhyodacitic melt inclusions are frequent in plagioclase, particularly in intrusive rocks (Fig. 8F), and quartz never contains melt inclusions with SiO_2 below 69 wt% (Fig. 8G). Amphibole and pyroxene contain some inclusions of andesitic composition, but a much larger number of more mafic inclusions (SiO_2 < 56 wt%). In intrusive rocks, there is virtually no compositional overlap between basaltic or andesitic melt inclusions in mafic phenocrysts and dacitic or more silica rich melt inclusions in plagioclase and quartz (Fig. 8B). Moreover, inclusions in plagioclase of intrusive rocks reach higher silica contents than do the most felsic inclusions in any of the volcanic rocks.

These contrasts between melt compositions enclosed in mafic and felsic phenocrysts become even more obvious when average melt inclusions and bulk rock compositions are compared for individual rocks (Fig. 9). With only two exceptions (samples NB9 and NB5B), the mafic minerals have trapped melts with lower average silica content than the host rock, whereas apparently co-existing felsic phenocrysts have trapped melts of a more acid composition. This consistent observation, and the commonly large contrasts between melt enclosed by different minerals, demonstrate that most of the seemingly coexisting phenocrysts cannot have crystallized together from the same melt.

Sulfide melt inclusions are widespread in amphibole of intrusive rocks, extremely rare in amphibole from volcanic rocks, but absent from other phases. Only two volcanic rocks, out of approximately 50 investigated in detail, contain magmatic sulfide inclusions. Primary sulfides have never been found in the matrix of either volcanic or intrusive rocks.

Interpretation and discussion

Geological evidence and compositional data of bulk rocks, phenocrysts and melt inclusions—in addition to constraints imposed by the presence of a large ore deposit and existing experimental data—confine the magmatic evolution in the Farallón Negro Volcanic Complex. The combination of data indicates that magmatic evolution in the complex was dominated almost exclusively by mixing between mafic and felsic magmas, whereas melt—crystal fractionation played a minor role during magma evolution in the upper crust. In situ crystallization influenced melt compositions only at a local scale. Our data constrain the compositions of the primary melts, the extent of mixing between these melts, and they allow some inferences about the structure and evolution of the subvolcanic magma chamber and the processes leading to eruption. Key to the following discussion is a clear distinction between melt and bulk magma compositions.

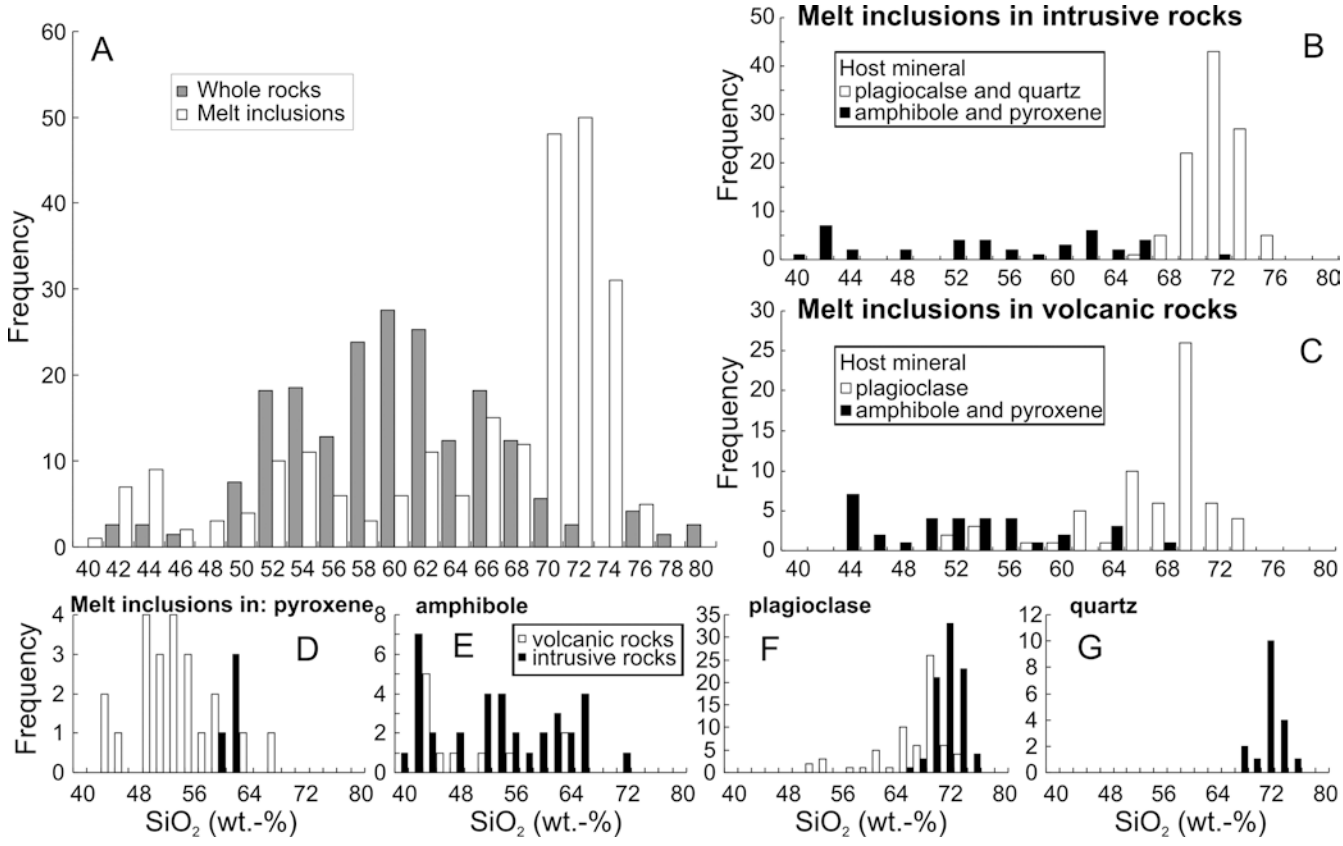

Fig. 8 Histogram of the frequency distribution of melt inclusions at various SiO_2 concentrations in all the samples (**A**), in intrusive (**B**) and extrusive (**C**) rocks and in amphibole (**D**), pyroxene (**E**), plagioclase (**F**) and quartz (**G**). In histograms comparing inclusions from various host phases, the frequency of inclusions was normalized to their abundance. These histograms clearly show that mafic phenocrysts crystallized from different melts than plagioclase and quartz. This is particularly pronounced for intrusive rocks where melt inclusions of similar composition are almost never recorded in mafic and felsic phases. Overall, melt inclusions are either mafic or silica-rich; melt inclusions of intermediate composition are rare, yet magmas of intermediate andesitic composition are volumetrically dominant

Magma mixing and the large-scale evolution

Tight and near-linear changes in bulk rock compositions in all major and most trace elements, extending from extremely mafic ($<45\%$ SiO_2) to rhyodacitic compositions ($>70\%$ SiO_2) is difficult to explain by fractional crystallization of the observed phenocryst phases (Halter et al. 2004a). Fractional crystallization with physical separation of crystals from the melt would generate curved trends (e.g., in Al_2O_3 or K_2O) depending on the stable phases and cannot explain the widespread observation of highly contrasting melt inclusion compositions in andesites with low phenocryst contents (Fig. 9). By contrast, mixing of two distinct magmas can explain linear variations in whole-rock compositions (shown by the black dashed lines in Fig. 5), as well as the more diagnostic evidence from the bimodal distribution of silicate melt inclusions. It is likely that the compositions of the mixing components were close to the most silica-poor melts (42–45 wt% SiO_2) and silica-rich melt inclusions (68–70 wt% SiO_2). The frequencies of bulk rock and melt inclusion compositions throughout the complex provide a clear indication that magma mixing occurred not only locally, but indeed is the volumetrically predominant crustal process controlling magma compositions in the FNVC.

Magma mixing in individual rock samples is also demonstrated by element co-variations within inclusions of one phenocryst type. A particularly clear example is sample NB32 containing petrographically indistinguishable amphibole-hosted melt inclusions spanning a compositional range from basaltic andesite to rhyodacite. Variations in the Al_2O_3, Sr, Rb and Y contents of the melt across this range of silica concentrations are inconsistent with amphibole fractionation (and, thus, exclude inappropriate host corrections). Instead, they demonstrate progressive mixing of two magmas during amphibole crystallization. Other strong evidence for mixing are melt inclusions of 66 to 68 wt% SiO_2 in plagioclase phenocrysts, themselves trapped in amphibole hosting inclusions with 50 wt% SiO_2(Fig. 4B), and by the bimodal distribution of melt inclusion chemistries (Fig. 8).

Additional striking evidence for mixing is indicated by melt inclusions trapped in amphibole and felsic minerals from intrusive rocks that hardly ever overlap in their silica content (Fig. 8), despite the widespread common occurrence of these phases. More generally,

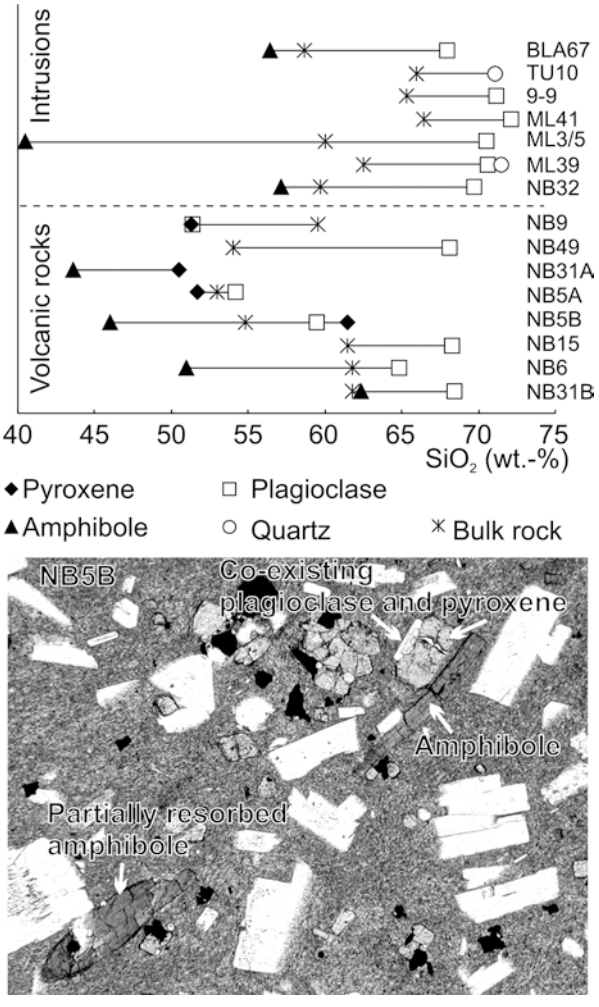

Fig. 9 Silica content of whole rocks and melt inclusions in different phenocrysts in the same sample. Within one samples, the range in inclusion composition in each phase is small and was averaged. Compositions of bulk rocks are generally intermediate between those of melt inclusions in amphibole and melt inclusions in plagioclase and quartz. This shows that different phenocrysts formed in chemically different melts, and that their association in a magma of intermediate composition is the result of mixing. The microphotograph shows the texture of one sample, in which plagioclase and pyroxene crystallized together and trapped compositionally similar inclusions, whereas earlier amphibole with more mafic inclusions is partially resorbed

melt inclusions have highly contrasting compositions in different phenocrysts from the same rock (Fig. 9) and, thus, phenocrysts do not represent stable equilibrium assemblages. Petrographically co-genetic pyroxene- and plagioclase-hosted melt inclusions with similar SiO_2contents only exist in samples NB9 and NB5A. In sample NB32, some amphiboles have melt inclusions similar to those trapped in plagioclase and are also considered to represent a stable assemblage (Halter et al. 2004b). For all the other rocks, the contrast in melt inclusion compositions (Fig. 9) suggests that phenocrysts formed in different melts and were mechanically mixed to generate the observed phase assemblage.

Crystallisation and local processes

The compositions of melt inclusions generally follow the same mixing line as bulk rocks, but in individual samples, distinct deviations from this mixing line are apparent. These deviations may be related to a particular process such as crystallization, volatile exsolution or sulfide saturation, which affect melt compositions and may generate some compositionally extreme residual melts.

Melt inclusions with SiO_2 contents in excess of 68 wt% are common in plagioclase and quartz. Equivalent bulk rock compositions are rare, indicating that melt inclusions represent local residual melts that were rarely separated from the crystals to intrude or extrude as distinct magma batches. Thus, crystallization in these magmas is more likely to occur without significant removal of solid phases from the melt. In line with this interpretation, the significant increase in the variability between samples of K_2O, Na_2O, Rb and Sr concentrations in silica-rich melt inclusions can be explained by local crystallization of phenocrysts. Indeed, the concentration of highly compatible or incompatible elements in a given mineral can be significantly affected by the crystallization of that mineral. This will result in contrasting compositions between the host rock and the melt, provided that the mineral is not removed. As a consequence, extreme melt compositions, such as very K-rich melts, can be generated by crystallization of K-poor phases. For instance, the crystallization of plagioclase from a melt with 64 wt% SiO_2 could raise the K_2O content from 3 to 7 wt% by the time the SiO_2 content reaches 70 wt% (Fig. 5, arrow 2). Such deviations of melt inclusion compositions from bulk rock trends are systematic in individual samples, but restricted to some specific rocks, suggesting that such processes were important only locally, i.e., affecting only small magma batches.

Primary silica-rich and silica-poor magmas had most likely undergone some crystallization prior to their mixing. In particular, melt inclusions in intrusive rocks appear to be more silica-rich than inclusions in volcanic rocks (Fig. 8), suggesting a higher degree of crystallization (mainly of plagioclase) in intrusions. This induces an increase of incompatible elements and a depletion of compatible elements in residual melts prior to mixing. As a consequence, the mixing lines for melts can deviate significantly from mixing lines of bulk rocks. For instance, a depletion of K in the residual melt of highly crystallized, felsic magma induced a lower K content in the mixed melt (colored dashed lines in Fig. 5). Thus, intermediate melts deviate from the composition of bulk rocks after mixing. This deviation is more pronounced in intrusive rocks, due to the high degree of plagioclase crystallization in the felsic magma prior to mixing. It cannot be explained by plagioclase crystallization from intermediate melts, as plagioclase does not appear to crystallize in melts with less than 68 wt% SiO_2 in intrusive magmas (plagioclase in intrusive rocks contain

abundant melt inclusions but only very few have intermediate composition). The same process accounts for the enrichment in Y, Rb or Sr in melt inclusions of intermediate SiO_2 contents.

The two end-member magmas

The two endpoints of the mixing line of bulk rock and melt inclusion compositions provide reasonable limiting estimates for endmember compositions of magmas involved in the mixing process. Some compositional variation of the primitive magmas is likely, but this variation cannot have been very large or systematic, because all rock compositions lie on the same mixing line, irrespective of age or mode of emplacement. Evidence for a constant composition of the most mafic magma is provided by constant compositions of the most mafic melt inclusions in amphiboles of rocks of various ages (Fig. 6). All deviations of melt inclusion compositions from the whole-rock mixing trend can be plausibly explained by local crystallization or volatile loss, indicating that no significant additional components are required.

The most mafic melts preserved in magnetite-bearing amphibole probably approximate the silica-poor endmember involved in the mixing process. The similarity in composition of these inclusions in intrusive and extrusive rocks (Fig. 6) suggests a common source for the mafic melt in both rock types. These melt inclusions are unusually poor in silica (42 to 45 wt%), but have similar major element compositions to olivine and pyroxene bearing shoshonitic lamprophyre dykes intruded early in the genesis of the complex (Halter et al. 2004a). These dykes show progressively decreasing mantle-normalized trace element patterns (Fig. 7), comparable to those described for basaltic andesites from various South American (e.g., Thorpe et al. 1982; Hickey et al. 1986) and North American (e.g., Grove et al. 2002) volcanoes. Melt inclusion patterns are flatter, indicating a more primitive composition than the lamprophyre dykes.

The silica-rich endmember of the mixing process probably had SiO_2 concentrations between 65 and 68 wt%. Melt with higher SiO_2 concentrations and anomalously high K_2O or Rb concentrations are interpreted to have been generated by crystallization of plagioclase in the magma. Melt inclusions with such SiO_2 contents are trapped in rocks at the base of the volcanic stratigraphy, indicating that these melts were indeed present throughout the history of the magmatic complex. Magmas of similar composition are only found as late intrusions, thus melt inclusions are the only record for the presence of silica-rich melt at an early stage.

The ultimate source of the silica-rich magma component is not identified, but it has a crustal component based on its Nd, Sr and Pb isotopic composition when compared with the most mafic rocks (Halter et al. 2004). In similar systems, partial melting of the crust (Grove et al. 1997; Sisson et al. 1996; Bacon and Druitt 1988; Bacon 1992) including older gabbroic rocks (Feeley et al. 1998), or residual melts from basalt crystallization in the lower crust (Annen et al. 2002), have been suggested as possible contributors. Such melts could be derived from melting in the lower crust and probably mixed with mafic melt before entering the magma chamber (with $\sim$68 wt% SiO_2).

Petrologic constraints on phenocryst evolution and magma emplacement

The application of equilibrium petrology as rigorous constraints on the petrogenesis of the FNVC is severely limited by the disequilibrium assemblages present in these rocks. As phenocrysts contain melt inclusions with contrasting compositions, they cannot represent true equilibrium assemblages. Within these restrictions, however, our textural and compositional data are consistent with experimental data.

According to Moore and Carmichael (1998), basaltic andesitic melts crystallize amphibole and Fe-oxides only at pressures above 350 MPa at water saturated conditions and temperatures of approximately 1,000 °C. The amount of water that can be dissolved in the melt at these conditions exceeds 6 wt%. We suggest that these are minimum values for pressure and water content during the formation of the most mafic melt inclusions in amphibole. True pressures and water contents might be even higher as the silica content of these melts is lower than in the experiments by Moore and Carmichael (1998). Thus, a large proportion of the volatiles present in the system could have been added by the mafic magma, and could ultimately be derived from a subducting slab.

Melts of intermediate compositions are trapped preferentially by plagioclase in volcanic rocks and by amphibole in intrusive rocks. In both cases, mixing appears to have occurred outside the stability field of pyroxene, as this phase does not record the high variability in melt compositions present in the other two minerals. As amphibole is the sole host for intermediate inclusions in intrusive rock, it is likely to be the only phase to crystallize in significant amounts during mixing. In extreme cases, high water content stabilized amphibole in melts with 70 wt% SiO_2 (sample NB32). In andesites, the coexistence of amphibole and plagioclase and the absence of pyroxene indicate water contents above 5.5 wt% and pressures in excess of 250 MPa (Moore and Carmichael 1998). A high water content during mixing is consistent with the systematic presence of sulfide melt inclusions in amphibole, suggesting that the magma did not extensively degas. Degassing would de-stabilize sulfides through the loss of sulfur to the volatile phase and suppress sulfide saturation.

In volcanic rocks, mixing is mainly recorded in plagioclase. Amphiboles rarely trap melt inclusions of intermediate composition suggesting that this phase was not stable during the mixing process that generated most

volcanic rocks. Very few sulfide inclusions were found in amphibole phenocrysts in the dominantly andesitic extrusive rocks, suggesting that these magmas never exsolved a sulfide melt on a broad scale. Degassing upon magma mixing likely suppressed the formation of a sulfide melt (Keith et al. 1997).

Evolution after mixing

Inclusions in pyroxene indicate that this phase is formed in melts with a restricted chemical range (SiO_2 contents between 50 and 55 wt%). Textural evidence and chemically similar melt inclusions show that pyroxene is crystallizing together with plagioclase from these melts (Fig. 9, sample NB5B; see also Fig. 6 in Halter et al. 2004b). Such inclusions were probably trapped after magma mixing and record the subsequent melt evolution. In rocks where pyroxene and plagioclase co-exist, amphibole is partially resorbed (Fig. 9), recording a shift from a plagioclase (±amphibole) stable assemblage to the plagioclase + pyroxene stability field. In water-saturated melts of intermediate composition, the latter assemblage is stable at pressures below 150 MPa and temperatures around 950 °C (Moore and Carmichael 1998). Thus, the replacement of amphibole by pyroxene and plagioclase is readily explained by the ascent of the magma towards the surface. The associated pressure drop causes concurrent degassing of the magma. Melt inclusions recording this event show enrichment in K_2O, consistent with crystallization of potassium-free plagioclase and pyroxene at the expense of amphibole (Fig. 9). The same combined effect induces a decrease in the silica content of the residual melt (arrow 1 in Fig. 5). Thus, upon ascent of the magma from an upper crustal reservoir to the surface, residual melt (not the magma) evolves towards more mafic compositions.

Structure and dynamics of an evolving magma chamber

We combine the chemical constraints from published experiments with our observations from bulk rocks and melt inclusions to propose a qualitative physical model for the evolution of the entire Farallón Negro Volcanic Complex. This evolution includes an initial build-up of a volcanic edifice over 2 million years, the gradual establishment of an internally structured magma chamber, and the final crystallization of this magma reservoir (Fig. 10). We emphasize the conclusion that different processes dominate in different regions of a single magmatic system that evolved over 3 m.y., by continued

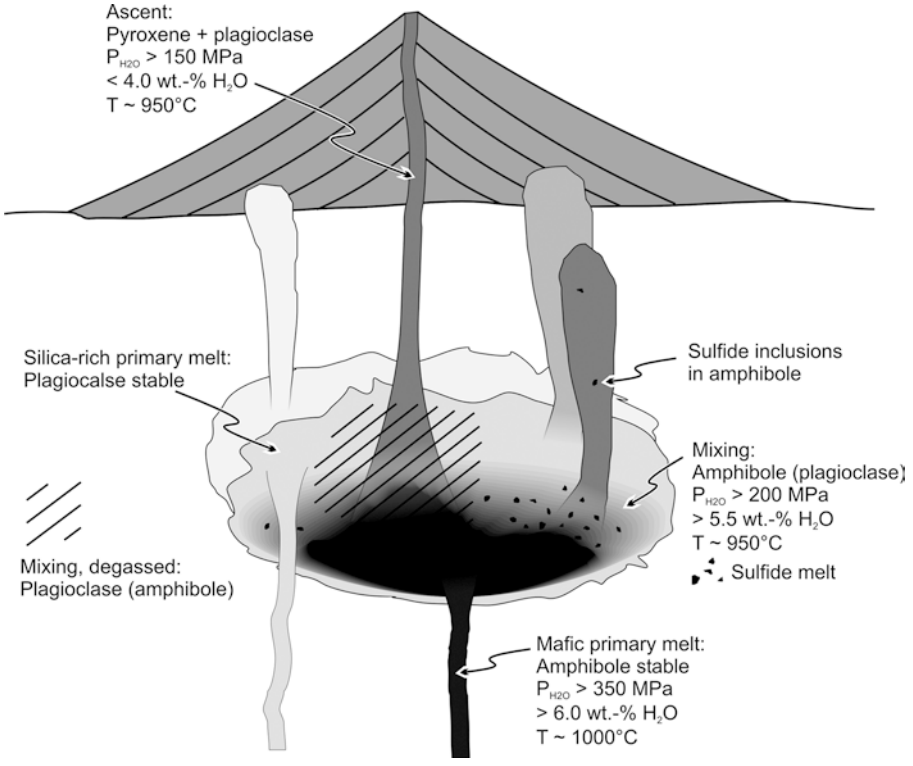

Fig. 10 Illustration summarizing inferred processes and possible structure of the magmatic system below the Farallón Negro Volcanic Complex. Based on melt inclusion data and phase equilibria, we suggest that the most mafic magma is water saturated at 1,000 °C and 350 MPa. This magma is mixed with a silica-rich magma in a gradually developing reservoir at approximately 950 °C and 250 MPa. During mixing, the magma saturated a fluid phase, which triggered eruption through the main volcanic conduit. Sulfide saturation occurred at the same time in parts of the magma reservoir from which subvolcanic intrusions were derived/extracted. Further degassing during ascent in the volcanic conduit was responsible for the replacement of amphibole by pyroxene and plagioclase at 150 MPa. Successive intrusions of progressively more mafic magmas in a single stock suggest that the magma chamber was layered

supply of two magmas of approximately constant composition.

Geological reconstruction of volcanic stratigraphy and numerous high-precision age data (Sasso 1997; Halter et al. 2004a) show an approximately steady extrusion rate of the order of 300 km^3 / Ma over an extended period of more than 2 m. y. During this period, volcanic rocks varied randomly between basalts and andesites, representing variable proportions of two magmas undergoing continued mixing. In the mafic magma, early amphibole and magnetite crystallized at high pressure (> 350 MPa) from melts close to, or at, water saturation (6.0 wt% H_2O). Plagioclase dominantly crystallized from the felsic magma endmember prior to mixing. Both magmas may have been at similar temperatures and viscosities, thanks to the high H_2O content of the mafic magma, which aids complete hybridization of the melts by preventing the mafic magma from rapid solidification (Sparks and Marshall 1986). Rapid changes in bulk rock chemistry suggest that no significant magma chamber was established in the first million years (Dungan et al. 2001). The absence of sulfides and the resorption of amphibole indicate that volcanic rocks were degassing upon mixing. This was probably a necessary process to drive eruptions, as neither the primitive mafic nor the felsic components did ever extrude. Mixing has been suggested as a trigger for eruption in several andesitic volcanoes (e.g., Pallister et al. 1996; Venezky and Rutherford 1997). In particular, the potential liberation of large amounts of SO_2 has been considered a key factor in major eruptions (Hattori 1993; Kress 1997).

Some 1.2 m. y. after initiation of extrusive activity, the continuous compositional evolution of subvolcanic intrusions with time can be taken as evidence for the gradual build-up and growth of a subvolcanic magma chamber (Fig. 3 and Halter et al. 2004a), heated by continued advection of magma through the center of the volcano. Characteristic differences between intrusive and extrusive rocks (Fig. 8), despite a common source (Fig. 6), show that intrusions tapped different parts of this magma chamber than did volcanic rocks. Source regions for intrusions were not actively degassed, causing amphibole to crystallize upon mixing. In the absence of intense degassing, emplacement of intrusions was likely caused by the buoyancy of silica- and volatile-rich magma in the roof zone of the magma chamber. In individual stocks, the evolution of successive intrusions from silica-rich to silica-poor magmas in a very short period of time is taken as evidence for a chemically structured magma chamber, with initial extraction of silica-rich melts from the top and progressively more mafic melt from deeper parts of the chamber.

Volcanic activity through the central feeder channel was terminated by the crystallization of the large Alto de la Blenda stock. Shortly after, the largest dacitic ignimbrite flow in the complex and the emplacement of its intrusive counterparts were associated with a partial caldera collapse at the northwestern end of the complex (Llambias 1972; Sasso 1997; Halter et al. 2004a). Cessation of volcanism was probably caused by the end of magma supply from beneath, concurrently ending the heat supply and forcing the system to progressively crystallize. Formation of the Bajo de la Alumbrera porphyry Cu-Au deposit started at 7.1 Ma, about 0.4 m. y. after the main volcanic activity had ceased. At this stage a minimum of ~7 km^3 of magma with ~200 ppm Cu (i.e., the Cu content of the most mafic melt inclusions) are required to source the total mass of Cu present in the ore deposit. This is less than the ≥23 km^3 estimated by Ulrich et al. (1999), but still requires a considerable magma reservoir by the time of ore formation. A fluid pressure of 110 MPa from fluid inclusions requires that a considerable volcanic edifice (> 3 km) was present at least during the early phase of the porphyry-related hydrothermal activity (Ulrich et al. 2002).

Conclusions and implications for the evolution of an andesitic complex

Reconstruction of the magmatic history of the ore-forming Farallón Negro Volcanic Complex shows a long-term and almost steady-state extrusive and barren intrusive activity through most of its 3 m. y. lifetime. This activity is terminated by a period of rapid crystallization and liberation of a massive amount of magmatic-hydrothermal ore fluid, which requires the presence of a moderate-sized magma chamber by that time (at least ~7 km^3). Subtle indications for the developing magma chamber are recorded by a continuous evolution of subvolcanic intrusions. No distinct evidence for the presence of a significant magma reservoir would be obtained from the extrusive rocks alone. As a consequence, our conclusions differ from those of detailed studies on otherwise comparable active andesitic volcanoes, which offer there no possibility to observe exposed evidence from intrusive rocks or from major hydrothermal ore deposits (Dungan et al. 2001).

Melt inclusions provide unambiguous evidence that nearly all intrusive and extrusive rocks in the FNVC result from the mixing of a dacitic and a hydrous basaltic to lamprophyric magma. Continued mixing as the volumetrically dominant process controlling magma chemistry is demonstrated by a predominance of magmas with intermediate andesitic composition, consistently carrying mafic and felsic phenocrysts generated from highly contrasting magmas. Hence, petrologic interpretations of mineral assemblages, such as pressure estimated from amphibole-plagioclase pairs, require caution, as they do not necessarily provide reliable information on equilibrium conditions during magma evolution. The rarity of bulk rocks approximating the two endmember magmas suggest that mixing is very rapid and effective, and probably even a necessary driving force for magma emplacement into the volcanic environment. Mixing of volatile-rich mafic with acidic melts can cause strong degassing, which potentially drives the eruption. The lack of massive degassing at the

roots of intrusions causes a sulfide liquid to exsolve and, thus, might be instrumental in the formation of the Alumbrera ore deposit (Halter et al. 2002a).

Acknowledgments The authors would like to thank Minera Alumbrera Ltd. and MIM Exploration for their logistic support during the field work required by this study. We would also like to thank John Dilles, Tim Grove, Jake Lowenstern, Steve Sparks, and Alan Thompson for extensive discussions about our observations and the presentation of this paper. Charles Mandeville, Eric Christiansen and an anonymous reviewer provided key suggestions to improve the manuscript and their help was greatly appreciated.

References

Allmendinger RW (1986) Tectonic development, southeastern border of the Puna plateau, Northwestern Argentine Andes. Geol Soc Am Bull 97:1070–1082

Annen C, Sparks RSJ, Blundy J (2002) Silicic melt generation by basalt crystallization in the deep crust. Geochim Cosmochim Acta 66:A23–A23

Bacon CR (1992) Partially melted granodiorite and related rocks ejected from Crater Lake caldera, Oregon. Trans R Soc Edinb Earth Sci 83:27–47

Bacon CR, Druitt TH (1988) Compositional evolution of the zoned calcalkaline magma chamber of Mount-Mazama, Crater Lake, Oregon. Contrib Mineral Petrol 98:224–256

Cline JS, Bodnar RJ (1991) Can economic porphyry copper mineralization be generated by a typical calc-alkaline melt. J Geophys Res Solid Earth Planet 96:8113–8126

Cole JW, Gamble JA, Burt RM, Carroll LD, Shelley D (2001) Mixing and mingling in the evolution of andesite-dacite magmas; evidence from co-magmatic plutonic enclaves, Taupo Volcanic Zone, New Zealand. Lithos 59:25–46

Coombs ML, Eichelberger JC, Rutherford MJ (2000) Magma storage and mixing conditions for the 1953–1974 eruptions of Southwest Trident Volcano, Katmai National Park, Alaska. Contrib Mineral Petrol 140:99–118

Coughlin TJ, O'Sullivan PB, Kohn BP, Holcombe RJ (1998) Apatite fission-track thermochronology of the Sierras Pampeanas, central western Argentina; implications for the mechanism of plateau uplift in the Andes. Geology (Boulder) 26:999–1002

Dietrich A, Lehmann B, Wallianos A, Traxel K (1999) Magma mixing in Bolivian tin porphyries. Naturwissenschaften 86:40–43

Dilles JH (1987) Petrology of the Yerington Batholith, Nevada—evidence for evolution of porphyry copper ore fluids. Econ Geol 82:1750–1789

Druitt TH, Bacon CR (1989) Petrology of the zoned calcalkaline magma chamber of Mount Mazama, Crater Lake, Oregon. Contrib Mineral Petrol 101:245–259

Dungan MA, Wulff A, Thompson R (2001) Eruptive stratigraphy of the Tatara-San Pedro complex, 36 degrees S, southern volcanic zone, Chilean Andes: reconstruction method and implications for magma evolution at long-lived arc volcanic centers. J Petrol 42:555–626

Feeley TC, Dungan MA, Frey FA (1998) Geochemical constraints on the origin of mafic and silicic magmas at Cordon El Guadal, Tatara-San Pedro Complex, central Chile. Contrib Mineral Petrol 131:393–411

Grove TL, DonnellyNolan JM, Housh T (1997) Magmatic processes that generated the rhyolite of Glass Mountain, Medicine Lake volcano, N California. Contrib Mineral Petrol 127:205–223

Grove TL, Parman SW, Bowring SA, Price RC, Baker MB (2002) The role of an H2O-rich fluid component in the generation of primitive basaltic andesites and andesites from the Mt. Shasta region, N California. Contrib Mineral Petrol 142:375–396

Halter WE, Bain N, Becker K, Heinrich CA, Landtwing M, VonQuadt A, Bissig T, Clark AH, Sasso AM, Tosdal RM (2004a) From andesitic volcanism to the formation of a porphyry-Cu-Au mineralizing magma chamber: the Farallón Negro Volcanic Complex, northwestern Argentina. J Volcanol Geotherm Res (in press)

Halter WE, Pettke T, Heinrich CA (2002a) The origin of Cu/Au ratios in porphyry-type ore deposits. Science 296:1844–1846

Halter WE, Pettke T, Heinrich CA (2004b) Laser-ablation ICP-MS analysis of silicate and sulfide melt inclusions in an andesitic complex I: analytical approach and data evaluation. Contrib Mineral Petrol

Halter WE, Pettke T, Heinrich CA, Rothen-Rutishauser B (2002b) Major to trace element analysis of melt inclusions by laser-ablation ICP-MS: methods of quantification. Chem Geol 183:63–86

Hattori K (1993) High-sulfur magma, a product of fluid discharge from underlying mafic magma—evidence from Mount-Pinatubo, Philippines. Geology 21:1083–1086

Heinrich CA, Pettke T, Halter WE, Aigner-Torres M, Audetat A, Gunther D, Hattendorf B, Bleiner D, Guillong M, Horn I (2003) Quantitative multi-element analysis of minerals, fluid and melt inclusions by laser-ablation inductively-coupled-plasma mass-spectrometry. Geochim Cosmochim Acta 67:3473–3497

Hickey RL, Frey FA, Gerlach DC, Lopezescobar L (1986) Multiple sources for basaltic arc rocks from the Southern Volcanic Zone of the Andes (34-Degrees-S-41-Degrees-S) - Trace-element and isotopic evidence for contributions from subducted oceanic-crust, mantle, and continental-crust. J Geophys Res Solid Earth Planet 91:5963–5983

Hofmann AW (1988) Chemical differentiation of the Earth—the relationship between mantle, continental-crust, and oceanic-crust. Earth Planet Sci Lett 90:297–314

Jaupart C, Tait S (1990) Dynamics of eruptive phenomena. Rev Miner 24:213–238

Jordan TE, Allmendinger RW (1986) The Sierra Pampeanas of Argentina: a modern analogue of Rocky Mountain foreland deformation. Am J Sci 260:737–764

Keith JD, Whitney JA, Hattori K, Ballantyne GH, Christiansen EH, Barr DL, Cannan TM, Hook CJ (1997) The role of magmatic sulfides and mafic alkaline magmas in the Bingham and Tintic mining districts, Utah. J Petrol 38:1679–1690

Kress V (1997) Magma mixing as a source for Pinatubo sulphur. Nature 389:591–593

Llambias EJ (1970) Geologia de los Yacimientos Mineros Agua de Dionisio, Prov. de Catamarca, Rep. Argentina. Revista de la Asociacion Argentina de Mineralogia Petrologia y Sedimentologia 1:2–32

Llambias EJ (1972) Estructura del grupo volcanico Farallon Negro, Catamarca, Republica Argentina. Revista de la Asociacion Geologica Argentina 27:161–169

Mandeville CW, Carey S, Sigurdsson H (1996) Magma mixing, fractional crystallization and volatile degassing during the 1883 eruption of Krakatau volcano, Indonesia. J Volcanol Geotherm Res 74:243–274

Martinez L, Meilán D, Maza AE (1995) Mapa geológico de la provincia de Catamarca, República Argentina. Secretaria de Minería, Dirección Nacional del Secvicio Geológico

Matthews SJ, Gardeweg MC, Sparks RSJ (1997) The 1984 to 1996 cyclic activity of Lascar volcano, northern Chile: cycles of dome growth, dome subsidence, degassing and explosive eruptions. Bull Volcanol 59:72–82

Moore G, Carmichael ISE (1998) The hydrous phase equilibria (to 3 kbar) of an andesite and basaltic andesite from western Mexico: constraints on water content and conditions of phenocryst growth. Contrib Mineral Petrol 130:304–319

Murphy MD, Sparks RSJ, Barclay J, Carroll MR, Brewer TS (2000) Remobilization of andesite magma by intrusion of mafic magma at the Soufriere Hills Volcano, Montserrat, West Indies. J Petrol 41:21–42

Pallister JS, Hoblitt RP, Meeker GP, Knight RJ, Siems DF (1996) Magma mixing at Mount Pinatubo; petrographic and chemical

evidence from the 1991 deposits. In: Newhall Christopher G, Punongbayan Raymundo S (eds) Fire and mud; eruptions and lahars of Mount Pinatubo, Philippines, Philippine Institute of Volcanology and Seismology, Quezon City, Philippines | University of Washington PressUnited States, pp 687–731

Pettke T, Webster JD, Halter WE, Heinrich CA, Aigner-Torres M, De Vivo B (2002) Advantages and limitations of quantifying melt inclusion chemistry by LA-ICPMS, EMP and SIMS. Geochim Cosmochim Acta 66:A596–A596

Proffett JM (1995) Geology of the Bajo de la Alumbrera porphyry copper-gold deposit, Catamarca province, Argentina. 2, Minera Alumbrera Internal Report

Sasso AM (1997) Geological evolution and metallogenetic relationships of the Farallon Negro volcanic complex, NW Argentina. PhD Thesis, Queen's University, Kingston, Ontario, 843 pp

Sigurdsson H, Sparks RSJ (1981) Petrology of rhyolitic and mixed magma ejecta from the 1875 eruption of Askja, Iceland. J Petrol 22:41–84

Sisson TW, Grove TL, Coleman DS (1996) Hornblende gabbro sill complex at Onion Valley, California, and a mixing origin for the Sierra Nevada batholith. Contrib Mineral Petrol 126:81–108

Sparks RSJ, Marshall LA (1986) Thermal and mechanical constraints on mixing between mafic and silicic magmas. J Volcanol Geotherm Res 29:99–124

Stix J, Torres R, Narvaez L, Cortes GP, Raigosa J, Gomez D, Castonguay R (1997) A model of vulcanian eruptions at Galeras volcano, Colombia. J Volcanol Geotherm Res 77:285–303

Tait S, Jaupart C, Vergniolle S (1989) Pressure, gas content and eruption periodicity of a shallow, crystallizing magma chamber. Earth Planet Sci Lett 92:107–123

Thorpe RS, Francis PW, Hammill M, Baker MCW (1982) The Andes. In: Thorpe RS (ed) Andesites; orogenic andesites and related rocks. Wiley, Chichester, pp 187–205

Ulrich T, Gunther D, Heinrich CA (1999) Gold concentrations of magmatic brines and the metal budget of porphyry copper deposits. Nature 399:676–679

Ulrich T, Gunther D, Heinrich CA (2002) Evolution of a porphyry Cu-Au deposit, based on LA-ICP-MS analysis of fluid inclusions: Bajo de la Alumbrera, Argentina (vol 96, pp 1743, 2001). Econ Geol Bull Soc Econ Geol 97:1888–1920

Ulrich T, Heinrich CA (2002) Geology and alteration geochemistry of the porphyry Cu-Au deposit at Bajo de la Alumbrera, Argentina (vol 96, pp 1719, 2001). Econ Geol Bull Soc Econ Geol 97:1863–1888

Urreiztieta M, Rosello EA, Gapais D, LeGorve C, Cobbold PR (1993) Neogene dextural transpression at the southern edge of the Altiplano-Puna (NW Argentina), II International Symposium on Andean Tectonics, Oxford, pp 267–269

Venezky DY, Rutherford MJ (1997) Preeruption conditions and timing of dacite-andesite magma mixing in the 2.2 ka eruption at Mount Rainier. J Geophys Res-Solid Earth 102:20069–20086

Wolf KJ, Eichelberger JC (1997) Syneruptive mixing, degassing, and crystallization at Redoubt Volcano, eruption of December, 1989 to May 1990. J Volcanol Geotherm Res 75:19–37